

# Weak Hydrogen Bridges: A Systematic Theoretical Study on the Nature and Strength of C–H...F–C Interactions

Isabella Hyla-Kryspin,\* Günter Haufe, and Stefan Grimme\*[a]

**Abstract:** We present a comparative study on the nature and strength of weak hydrogen bonding between the C(sp<sup>3</sup>)–H, C(sp<sup>2</sup>)–H, and C(sp)–H donor bonds and F–C(sp<sup>3</sup>) acceptors. The series of molecules CH<sub>3</sub>F·CH<sub>4</sub> (**2a**, **2b**), CH<sub>3</sub>F·C<sub>2</sub>H<sub>4</sub> (**3**), CH<sub>3</sub>F·C<sub>2</sub>H<sub>2</sub> (**4**), as well as model complexes of experimentally characterized 2-fluoro-2-phenylcyclopropane derivatives, C<sub>3</sub>H<sub>6</sub>·C<sub>3</sub>H<sub>5</sub>F (**5a**, **5b**) and C<sub>3</sub>H<sub>5</sub>F·C<sub>3</sub>H<sub>5</sub>F (**6**) were investigated. Comparative studies were also performed for two conformers of the methane dimer (**1a**, **1b**). The calculations were carried out in hierarchies of basis sets [SV(d,p), TZV(d,p), aug-TZV(d,p), TZV(2df,2pd), aug-TZV(2df,2pd), QZV(3d2fg,2pd), aug-QZV(3d2fg,2pdf)] by means of ab

initio [HF, MP2, QCISD, QCISD(T)] methods and density functional theory (DFT/B3LYP, DFT/PBE). It is shown that well-balanced basis sets of at least TZV(2df,2pd) quality are needed for a proper description of the weakly bonded systems. In the case of **2**, **3**, **5**, and **6**, the dispersion interaction is the dominant term of the entire attraction, which is not accounted for at the B3LYP level. Significant electrostatic contributions are observed for **6** and **3**.

**Keywords:** ab initio calculations · density functional calculations · fluorinated cyclopropanes · hydrogen bridges · weak hydrogen bonding

For **4**, these forces have a dominating contribution to the hydrogen bonding. The C(sp)–H...F–C(sp<sup>3</sup>) interaction in **4**, though weak, exhibits the same characteristics as conventional hydrogen bridges. Despite showing longer H...F/H contacts compared to **1a**, **2a**, and **5a** the bifurcated structures, **1b**, **2b**, **5b**, are characterized by larger dispersion interactions leading to stronger bonding. For the systems with only one H...F contact, the MP2/QZV(3d2fg,2pd) interaction energy increases in the order **2a** (–1.62 kJ mol<sup>–1</sup>), **3** (–2.79 kJ mol<sup>–1</sup>), **5a** (–5.97 kJ mol<sup>–1</sup>), **4** (–7.25 kJ mol<sup>–1</sup>), and **6** (–10.02 kJ mol<sup>–1</sup>). This contradicts the estimated proton donor ability of the C–H bonds (**2a** < **5a** < **3** < **6** < **4**).

## Introduction

The hydrogen bonding defined in the standard formulation as a X–H...Y interaction, where X–H is the proton-donating covalent polar bond and Y is the proton-accepting group, belongs to one of the most important concepts in chemistry. It provides an explanation of conformational preferences of molecules, their properties, and reactivities in the gas, liquid, and solid phases.<sup>[1]</sup> For conventional or strong hydrogen bonds, both X and Y are electronegative atoms, such as O, N, or F. On the basis of a huge amount of convincing information, both theoretical and experimental, this type of bonding is quite well understood, nowadays. The commonly accepted criteria for the existence of hydrogen bonds are related to energetic, structural, and spectroscopic properties of the interacting species. The binding energies (BEs) of strong

hydrogen bonds are normally larger than ≈20 kJ mol<sup>–1</sup> and the distance between the proton and the acceptor atom (H...Y) is significantly shorter than the sum of their van der Waals radii.<sup>[2]</sup> A red shift of the stretching vibration of the proton-donating bond is usually observed in the corresponding IR spectra. It correlates with the X–H bond length and the H...Y bond strength.<sup>[2,3]</sup> Furthermore, NMR chemical shifts, their anisotropy, and through-space spin–spin couplings are also indicative for the existence of hydrogen bonding.<sup>[2,4]</sup> For unusually activated donors and acceptors, as in the case of the “inorganic” fluoride ion F–H...F<sup>–</sup>, and the charged O–H...O<sup>–</sup>, N<sup>+</sup>–H...N or O<sup>+</sup>–H...O systems, there is very strong hydrogen bonding, whose energy and nature shows similarities to covalent bonds.<sup>[5]</sup> On the other hand, for systems in which both X and Y or only one of them, are of moderate-to-low electronegativity, the bond energies drop significantly below 20 kJ mol<sup>–1</sup> and approach values typical of van der Waals interactions (weak hydrogen bonds).<sup>[2,6]</sup> For this type of interaction, a return to the term “hydrogen bridge” was recommended.<sup>[2c]</sup> Thus, one may distinguish between systems with 1) weak donors and strong acceptors, for example, C–H...N/O,<sup>[7,8]</sup> 2) strong donors and

[a] Dr. I. Hyla-Kryspin, Prof. Dr. G. Haufe, Prof. Dr. S. Grimme  
Organisch-Chemisches Institut der Universität Münster  
Corrensstrasse 49, 48149 Münster (Germany)  
Fax: (+49) 251-8336515  
E-mail: ihk@uni-muenster.de  
grimmes@uni-muenster.de

weak acceptors, such as O/N–H...F–C,<sup>[9,10]</sup> and 3) weak donors and weak acceptors, such as C–H...F–C<sup>[11]</sup> or C–H... $\pi$ <sup>[12]</sup> systems. Agostic interactions and dihydrogen bonds, X–H <sup>$\delta^+$</sup> ... $\delta^-$ –H–M, where X–H is the typical proton donating group with an electronegative X atom and M–H is the metal-hydride  $\sigma$  bond are also classified as weak hydrogen-bonded systems.<sup>[13,2a]</sup> Contrary to conventional hydrogen bonds, a shortening of the proton-donating bond and a blue shift of its stretching vibration is often observed in the IR spectra of weak hydrogen bridges.<sup>[12d]</sup> Theoretically, one way to characterize hydrogen bond systems is based on the topological analysis of the electron density, that is, on the AIM method.<sup>[14a]</sup> Recent investigations showed that the proposed criteria for the existence of hydrogen bonds according to the topological analysis of the electron density<sup>[14b–d]</sup> are also satisfied in the case of weak hydrogen bridges exhibiting the blue shift.<sup>[12d]</sup>

Based on Cambridge Structural Database (CSD) studies for a set of molecules containing C, H, and F with H...F contacts shorter than 2.8 Å, Shimoni and Glusker recognized that a fluorine atom covalently linked to a carbon atom (so-called “organic” fluorine) is a very poor hydrogen-bond acceptor and even poorer than the less electronegative oxygen or nitrogen atoms in analogous O–C or N–C bonds.<sup>[15]</sup> The authors revealed that attractive C–H...F–C interactions occur, but they are very weak.<sup>[15]</sup> Because of the importance of fluorine in biochemical environments and the common practice to replace a hydrogen atom or hydroxyl group by fluorine to generate a fluorinated enzyme substrate or inhibitor in a given enzymatic process,<sup>[16]</sup> subsequent CSD searches were carried out with more severe criteria for the F...H distance.<sup>[17]</sup> According to a CSD analysis of Howard et al. with  $R_{\text{H...F}} < 2.35$  Å, short C–H...F–C contacts occur somewhat more frequently than O/N–H...F–C hydrogen bonds, but they are still relatively rare.<sup>[17a]</sup> On the basis of a similar CSD study with  $R_{\text{H...F}} < 2.3$  Å, Dunitz and Taylor concluded that short contacts between covalently bound fluorine and OH or NH groups are extremely rare and that only a few structures may be classified as exhibiting true hydrogen bonds.<sup>[17b]</sup> However, other authors regarded a distance of about the sum of van der Waals radii (2.67 Å)<sup>[18]</sup> or even longer to be hydrogen bonds.<sup>[2b,11c,19]</sup> Furthermore, the recent synthesis and structural characterization of 2-fluoro-2-phenylcyclopropane derivatives revealed that, in addition to C–H...F–C distances which are close to or slightly below the sum of the van der Waals radii, very short H...F distances, that is, below 2.3 Å, are observed in the crystal structures of these species.<sup>[11d]</sup>

This work presents a comprehensive study of the nature and magnitude of the C–H...F–C interaction in several model systems, which may be regarded as controversial in the light of the aforementioned studies. Similarly to conventional hydrogen bridges, the strength and nature of weak hydrogen bridges should be inherently connected to the subtle balance between the Lewis acidity of the proton-donating bond and the Lewis basicity of the acceptor. We thus started our studies with a set of small systems, including CH<sub>4</sub>·CH<sub>4</sub> (**1**), CH<sub>4</sub>·FCH<sub>3</sub> (**2**), C<sub>2</sub>H<sub>4</sub>·FCH<sub>3</sub> (**3**), and C<sub>2</sub>H<sub>2</sub>·FCH<sub>3</sub> (**4**). The choice of **2–4** should allow us to follow how the enhanced

acidity of the C–H donor bond effects the nature of the C–H...F–C interaction. The methane dimer (**1**), in which the intermolecular attraction is dominated by dispersion, was chosen for the comparison. We then continue with model cyclopropane systems C<sub>3</sub>H<sub>6</sub>·C<sub>3</sub>H<sub>5</sub>F (**5**) and C<sub>3</sub>H<sub>5</sub>F·C<sub>3</sub>H<sub>5</sub>F (**6**) for experimentally characterized monofluorinated phenylcyclopropane derivatives<sup>[11d]</sup> which are compared to **1–4**.

As the hydrogen bonding becomes weaker and approaches typical van der Waals interaction energies, an unequivocal characterization of the interaction is no longer possible and thus, several controversial debates can be found in the literature.<sup>[20]</sup> This was also one of the main topics discussed during the recently held International Symposium *Fluorine in the Life Sciences*.<sup>[20f]</sup> Electrostatic contributions are dominant in strong hydrogen bridges, while charge transfer is most important for the strongest bonded systems from the top end of the hydrogen-bonding scale. In weak hydrogen bridges, the electrostatic term is relatively small and can be of the same magnitude or even smaller than the dispersion term.<sup>[8c]</sup> Theoretically, the dispersion contributions can be separated from the other terms by the comparison of results from Hartree–Fock calculations with those obtained by *ab initio* methods including electron correlation. To correctly characterize the nature of the C–H...F–C interactions and to provide conclusive answers, the calculations presented here were carried out within hierarchies of methods and with the basis sets described in the next section.

## Computational Details

All calculations were carried out with the TURBOMOLE system of programs.<sup>[21]</sup> As quantum chemical methods, Hartree–Fock (HF), second-order Møller–Plesset perturbation theory (MP2),<sup>[22]</sup> and density functional theory (DFT) employing hybrid B3LYP<sup>[23]</sup> and pure PBE<sup>[24]</sup> functionals were used. The MP2 calculations were carried out with the resolution of the identity technique (RIMP2)<sup>[25]</sup> and excluding the correlation of the 1s electrons of carbon and fluorine. Although MP2 is generally considered to be a relatively accurate method to account for dispersive interactions, it is well-known that it overestimates the effect quite often, as for example in the case of the pure van der Waals interaction in the benzene dimer.<sup>[26a]</sup> On the other hand, the complete basis set estimate for the MP2 binding energy of the water dimer is underestimated by  $\approx 2$  kJ mol<sup>-1</sup> compared to the experimental value.<sup>[26b]</sup> To clarify this point for the C–H...F–C interaction and estimate the MP2 errors, comparative calculations at the QCISD and QCISD(T) levels<sup>[27]</sup> were also carried out for **1–4** with the RICC program.<sup>[28]</sup>

The two DFT functionals were chosen for the following reasons. First, B3LYP is the most popular functional with a good performance for a wide range of ground state properties. Although B3LYP almost completely fails for the description of pure van der Waals bonded systems,<sup>[29]</sup> it is still in common use for weakly bonded ones. On the other hand, the pure (nonhybrid) PBE functional accounts, at least qualitatively, for dispersion forces and it is thus one aim of this study to explore the capabilities of both functionals for the different F...H interactions investigated in this work.

The accurate description of dispersive interactions requires an accurate description of the polarizabilities of the fragments, and this is only possible with large basis sets that include diffuse functions with small exponents. To reduce the basis set superposition error (BSSE), which leads to an artificial increase of the calculated binding energy (BE), appropriate polarization functions are also necessary. The BSSE was calculated according to the counterpoise (CP) method of Boys and Bernardi,<sup>[30]</sup> and

yields the final counterpoise-corrected binding energies (CPBE). The determination of the BSSE may also provide some insight into the quality of the basis set used in the calculations. The basis sets used here are: SVP, TZVP, aug-TZVP, TZVPP, aug-TZVPP, QZVPPP, and aug-QZVPPP.<sup>[21,31]</sup> For the sake of clarity, the number of primitive Gaussians together with the contraction schemes are presented in Table 1. The last column in Table 1 shows the number of contracted AO basis functions for the largest system studied, namely, C<sub>3</sub>H<sub>5</sub>F·C<sub>3</sub>H<sub>5</sub>F (**6**).

Table 1. Primitive Gaussians and contraction schemes of the AO basis sets used<sup>[21,31]</sup> together with the total number of the contracted AO basis functions for **6**.

| Basis set <sup>[a]</sup>         | C, F  | H                                | AOs<br>( <b>6</b> ) |
|----------------------------------|---|----------------------------------|---------------------|
| SVP ≡ SV(d,p)                    | (7s4p1d)/[3s2p1d]                           | (4s1p)/[2s1p]                    | 162                 |
| TZVP ≡ TZV(d,p)                  | (11s6p1d)/[5s3p1d]                          | (5s1p)/[3s1p]                    | 212                 |
| aug-TZVP ≡ aug-TZV(d,p)          | {(11s6p1d) + (1s1p1d)}/[6s4p2d]             | {(5s1p) + (1s1p)}/[4s2p]         | 324                 |
| TZVPP ≡ TZV(2df,2pd)             | (11s6p2d1f)/[5s3p2d1f]                      | (5s2p1d)/[3s2p1d]                | 388                 |
| aug-TZVPP ≡ aug-TZV(2df,2pd)     | {(11s6p2d1f) + (1s1p1d)}/[6s4p3d1f]         | {(5s2p1d) + (1s1p)}/[4s3p1d]     | 500                 |
| QZVPPP ≡ QZV(3d2fg,2pd)          | (11s7p3d2f1g)/[6s4p3d2f1g]                  | (6s2p1d)/[3s2p1d]                | 588                 |
| aug-QZVPPP ≡ aug-QZV(3d2fg,2pdf) | {(11s7p3d2f1g) + (1s1p1d1f1g)}/[7s5p4d3f2g] | {(6s2p1d) + (1p1d1f)}/[4s3p2d1f] | 948                 |

[a] The prefix “aug-” means that diffuse functions, as indicated in the second and third column, are added.

The smaller sets (SVP, TZVP) are included in this study in order to explore their performance, which may be of importance in future studies on much larger systems where the big basis sets become computationally too demanding. For example, in the case of **6**, which is only a model system, the QZVPPP basis comprises almost 600 contracted AOs. For the RIMP2 calculations we used the corresponding auxiliary basis sets from the TURBOMOLE library.<sup>[21,32]</sup> According to prior experience, errors resulting from the RI approximation are less than 0.05 kJ mol<sup>-1</sup> for BE and negligible for the optimized structural parameters. The geometries of **1–6** were optimized at the HF, B3LYP, and MP2 levels by the use of all the basis sets mentioned. In the case of **5** and **6**, optimizations with the aug-QZVPPP basis were omitted. If not mentioned otherwise, the calculated BE, BSSE, and CPBE values refer to the geometry corresponding to the actual basis set/method combination. To estimate how the BSSE influences the H···F distance, HF, MP2, DFT/PBE, and DFT/B3LYP potential energy curves (PEC) were calculated for **2–4**. In these calculations, only the TZVPP basis set and fixed MP2/TZVPP optimized structures were used.

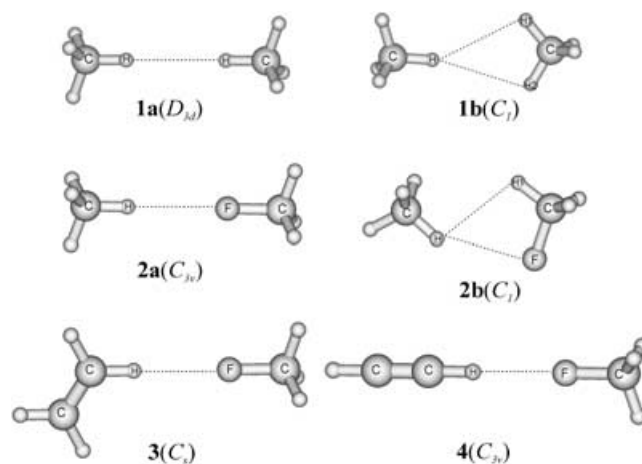
Theoretically, intermolecular interaction energies can be (arbitrarily) decomposed into chemically meaningful quantities, for example, electrostatics, polarization, exchange-repulsion, charge-transfer, and dispersion.<sup>[33]</sup> The most consistent way to calculate these quantities accurately is the symmetry-adapted perturbation theory (SAPT) approach.<sup>[34]</sup> For weak hydrogen bonds (and also from the viewpoint of the quantum-chemical methodology), the dispersion term is of particular importance. Thus, in this first work, we decided to employ a simplified scheme which nonetheless allows deep insight into the nature of bonding. We used the ratio between Hartree–Fock and MP2 interaction energies CPBE(HF)/CPBE(MP2) as a measure of the importance of the dispersion contributions. For simplicity, the first four contributions to the binding energy mentioned above, which are relatively accurately covered by the HF methods, are summarized in the following under the term “electrostatic contribution”. Coupling terms, which arise because electron correlation changes the properties of the monomers (e.g. their dipole moments), may have some effect for the contribution of pure electrostatics; however, they are not expected to influence our general conclusion regarding a series of structurally similar molecules.

Two additional points that are of particular importance for weak interactions will be also addressed in our work: the first one concerns the estimation of the complete basis set (CBS) limit for the MP2 interaction energies. These calculations were carried out for **2a**, **3**, and **4** with the aug-cc-pVXZ (X = 3, 4) basis sets<sup>[35]</sup> by means of the two-point approximation<sup>[36]</sup> for the uncorrected and counterpoise-corrected MP2 correlation

energy part. The second point concerns the shifts of the stretching vibrations of the C–H proton-donating bond. These investigations were carried out for the B3LYP/QZVPPP- and MP2/QZVPPP-optimized structures of **2a**, **3**, **4**, **6**, and the corresponding monomers. Harmonic vibrations were calculated with the SNF program.<sup>[37]</sup>

## Results and Discussion

**C–H···F–C interactions in compounds 2–4:** The calculations for molecules **1–4** were carried out for the conformations shown in Scheme 1. Important geometrical parameters of **1–4** together with binding energies (BE) and the basis set superposition errors (BSSE) are collected in Table 2 and Table 3. The counterpoise-corrected binding energies (CPBE) and the BSSE as a function of the basis set



Scheme 1. Molecular structures of the complexes **1–4**.

and method are depicted in Figure 1. The optimized H···F distances of **2a**(C<sub>3v</sub>), **3**(C<sub>s</sub>), and **4**(C<sub>3v</sub>) are compared in Figure 2. From Table 2, Table 3, and Figure 1, it is evident that the smallest SVP basis is not appropriate for these weakly bonded systems. For **1a**, **2a**, **1b**, and **2b**, independently of the method, the BSSE calculated with the SVP basis is nearly equal to or even larger than the binding energy itself. This situation is slightly better for the more strongly bound systems **3** and **4**, for which the BSSE corrections to the binding energies range from 32% (HF: **4**) to 88% (B3LYP: **3**).

As expected, the BSSE errors decrease systematically with increasing size of the basis set. For **2a**, **2b**, **3**, and **4** with the TZVP basis set, the BSSE corrections are 23–58% (MP2), 15–63% (B3LYP) and 8–45% (HF) of the corresponding binding energies. For the aug-QZVPPP basis set, these corrections diminish to 9–20% (MP2), 1–12%

Table 2. Optimized H–F bond lengths [ $\text{\AA}$ ] and C–H–F bond angles [ $^\circ$ ] as well as calculated binding energies (BE) [ $\text{kJ mol}^{-1}$ ] and basis set superposition errors (BSSE) [ $\text{kJ mol}^{-1}$ ] for  $\text{CH}_4\text{-CH}_4$  (**1a**( $D_{3d}$ )),  $\text{CH}_3\text{F-CH}_4$  (**2a**( $C_{3v}$ )),  $\text{CH}_3\text{F-C}_2\text{H}_4$  (**3**), and  $\text{CH}_3\text{F-C}_2\text{H}_2$  (**4**).

| Method/basis set | <b>1a</b> ( $D_{3d}$ ) |           |      | <b>2a</b> ( $C_{3v}$ ) |       |      | <b>3</b> ( $C_s$ ) |       |      | <b>4</b> ( $C_{3v}$ ) |        |      |
|------------------|------------------------|-----------|------|------------------------|-------|------|--------------------|-------|------|-----------------------|--------|------|
|                  | $R_{\text{H-H}}$       | BE        | BSSE | $R_{\text{H-F}}$       | BE    | BSSE | $R_{\text{H-F}}$   | BE    | BSSE | $R_{\text{H-F}}$      | BE     | BSSE |
| HF/SVP           | 3.470                  | -0.02     | 0.08 | 2.720                  | -2.42 | 2.24 | 2.601              | -3.81 | 2.52 | 2.278                 | -9.52  | 3.07 |
| B3LYP/SVP        | 2.722                  | -0.27     | 0.54 | 2.463                  | -5.39 | 5.42 | 2.364              | -6.84 | 5.99 | 2.139                 | -12.91 | 7.26 |
| MP2/SVP          | 2.522                  | -1.37     | 1.18 | 2.494                  | -5.04 | 4.56 | 2.415              | -6.58 | 5.03 | 2.185                 | -12.14 | 6.08 |
| HF/TZVP          | 3.213                  | not bound |      | 2.945                  | -0.82 | 0.37 | 2.748              | -2.01 | 0.44 | 2.353                 | -6.94  | 0.57 |
| B3LYP/TZVP       | 2.723                  | not bound |      | 2.720                  | -1.16 | 0.73 | 2.522              | -2.41 | 0.87 | 2.235                 | -7.52  | 1.15 |
| MP2/TZVP         | 2.725                  | -0.55     | 0.30 | 2.651                  | -2.29 | 1.20 | 2.496              | -3.87 | 1.65 | 2.266                 | -8.56  | 1.98 |
| HF/aug-TZVP      | 3.471                  | not bound |      | 3.115                  | -0.47 | 0.05 | 2.841              | -1.49 | 0.10 | 2.394                 | -5.83  | 0.18 |
| B3LYP/aug-TZVP   | 2.723                  | not bound |      | 2.723                  | -0.43 | 0.15 | 2.589              | -1.43 | 0.20 | 2.269                 | -5.84  | 0.36 |
| MP2/aug-TZVP     | 2.722                  | -1.91     | 1.36 | 2.522                  | -3.40 | 1.87 | 2.415              | -5.11 | 2.40 | 2.229                 | -9.31  | 2.39 |
| HF/TZVPP         | 3.213                  | not bound |      | 3.042                  | -0.67 | 0.26 | 2.783              | -1.70 | 0.34 | 2.389                 | -6.15  | 0.47 |
| B3LYP/TZVPP      | 2.723                  | not bound |      | 2.720                  | -0.91 | 0.51 | 2.560              | -1.90 | 0.74 | 2.259                 | -6.56  | 0.94 |
| MP2/TZVPP        | 2.718                  | -0.67     | 0.22 | 2.596                  | -2.26 | 0.87 | 2.464              | -3.62 | 1.12 | 2.215                 | -8.27  | 1.56 |
| HF/aug-TZVPP     | 3.213                  | not bound |      | 3.043                  | -0.49 | 0.06 | 2.849              | -1.49 | 0.10 | 2.388                 | -5.91  | 0.18 |
| B3LYP/aug-TZVPP  | 2.723                  | not bound |      | 2.721                  | -0.44 | 0.12 | 2.626              | -1.45 | 0.17 | 2.260                 | -5.95  | 0.35 |
| MP2/aug-TZVPP    | 2.717                  | -1.02     | 0.44 | 2.522                  | -2.51 | 0.81 | 2.415              | -4.26 | 1.32 | 2.186                 | -9.07  | 1.85 |
| HF/QZVPPP        | 3.213                  | not bound |      | 3.043                  | -0.51 | 0.08 | 2.837              | -1.51 | 0.13 | 2.391                 | -5.89  | 0.20 |
| B3LYP/QZVPPP     | 2.723                  | not bound |      | 2.721                  | -0.59 | 0.24 | 2.581              | -1.61 | 0.32 | 2.260                 | -6.10  | 0.45 |
| MP2/QZVPPP       | 2.723                  | -0.54     | 0.06 | 2.596                  | -1.96 | 0.34 | 2.418              | -3.30 | 0.51 | 2.218                 | -7.93  | 0.68 |
| HF/aug-QZVPPP    | 3.214                  | not bound |      | 3.044                  | -0.45 | 0.03 | 2.837              | -1.43 | 0.05 | 2.384                 | -5.78  | 0.08 |
| B3LYP/aug-QZVPPP | 2.724                  | not bound |      | 3.053                  | -0.34 | 0.04 | 2.606              | -1.32 | 0.04 | 2.270                 | -5.69  | 0.08 |
| MP2/aug-QZVPPP   | 2.723                  | -0.95     | 0.34 | 2.596                  | -2.44 | 0.48 | 2.419              | -3.81 | 0.58 | 2.193                 | -8.52  | 0.80 |

Table 3. Optimized H–H/F bond lengths [ $\text{\AA}$ ] and C–H–H/F bond angles [ $^\circ$ ] as well as calculated binding energies (BE) [ $\text{kJ mol}^{-1}$ ] and basis set superposition errors (BSSE) [ $\text{kJ mol}^{-1}$ ] for  $\text{CH}_4\text{-CH}_4$  (**1b**( $C_i$ )) and  $\text{CH}_3\text{F-CH}_4$  (**2b**( $C_i$ )).

| <b>1b</b> ( $C_i$ )<br>Method/basis | <b>2b</b> ( $C_i$ )                 |             | $\angle \text{CHH1} / \angle \text{CHH2}$ | BE        | BSSE | $R_{\text{H-F}} / R_{\text{H-H1}}$ | $\angle \text{CHF} / \angle \text{CHH1}$ | BE    | BSSE |
|-------------------------------------|-------------------------------------|-------------|---|-----------|------|------------------------------------|--|-------|------|
|                                     | $R_{\text{H-H1}} / R_{\text{H-H2}}$ |             |   |           |      |                                    |  |       |      |
| HF/SVP                              | 3.354/3.350                         | 155.1/174.0 |   | -0.03     | 0.13 | 2.695/3.195                        | 176.8/138.2                              | -3.78 | 3.87 |
| B3LYPSVP                            | 3.039/2.992                         | 168.8/156.5 |   | -0.13     | 0.50 | 2.449/2.993                        | 178.5/136.0                              | -7.93 | 8.10 |
| MP2/SVP                             | 2.755/2.767                         | 158.5/163.7 |   | -1.35     | 1.19 | 2.471/2.669                        | 174.4/128.1                              | -8.31 | 8.08 |
| HF/TZVP                             | 3.380/3.380                         | 156.9/172.4 |   | not bound |      | 3.020/3.825                        | 176.8/145.6                              | -0.76 | 0.30 |
| B3LYP/TZVP                          | 3.149/3.099                         | 165.5/161.4 |   | not bound |      | 2.721/3.561                        | 177.4/142.9                              | -1.25 | 0.72 |
| MP2/TZVP                            | 2.711/2.730                         | 160.1/161.7 |   | -1.60     | 1.38 | 2.739/2.739                        | 141.1/97.9                               | -3.20 | 1.85 |
| HF/aug-TZVP                         | 3.310/2.309                         | 159.6/167.3 |   | not bound |      | 3.021/3.823                        | 176.7/145.5                              | -0.50 | 0.09 |
| B3LYP/aug-TZVP                      | 3.161/3.087                         | 178.3/148.6 |   | 0.36      | 0.05 | 2.721/3.557                        | 177.4/142.8                              | -0.46 | 0.11 |
| MP2/aug-TZVP                        | 2.663/2.654                         | 159.7/161.2 |   | -2.38     | 1.70 | 2.637/2.578                        | 146.2/100.5                              | -4.82 | 2.20 |
| HF/TZVPP                            | 3.483/3.510                         | 157.3/173.2 |   | not bound |      | 3.020/3.821                        | 176.9/145.7                              | -0.78 | 0.39 |
| B3LYP/TZVPP                         | 3.070/3.047                         | 166.8/159.3 |   | not bound |      | 2.707/3.527                        | 178.1/143.2                              | -1.23 | 0.85 |
| MP2/TZVPP                           | 2.745/2.726                         | 159.0/163.2 |   | -1.11     | 0.28 | 2.615/2.620                        | 148.6/100.3                              | -3.82 | 1.51 |
| HF/aug-TZVPP                        | 3.318/3.343                         | 158.5/170.8 |   | not bound |      | 3.020/3.821                        | 176.9/145.7                              | -0.47 | 0.08 |
| B3LYP/aug-TZVPP                     | 3.179/3.123                         | 167.7/159.2 |   | not bound |      | 2.721/3.557                        | 177.4/142.9                              | -0.44 | 0.07 |
| MP2/aug-TZVPP                       | 2.734/2.708                         | 161.9/160.0 |   | -1.63     | 0.54 | 2.637/2.600                        | 145.5/100.2                              | -3.97 | 1.06 |
| HF/QZVPPP                           | 3.394/3.389                         | 168.3/161.6 |   | not bound |      | 3.020/3.820                        | 176.9/145.7                              | -0.55 | 0.15 |
| B3LYP/QZVPPP                        | 3.084/3.032                         | 166.9/159.3 |   | not bound |      | 2.707/3.525                        | 178.0/143.2                              | -0.79 | 0.40 |
| MP2/QZVPPP                          | 2.794/2.799                         | 153.5/169.5 |   | -1.08     | 0.11 | 2.615/2.615                        | 148.5/103.2                              | -3.36 | 0.64 |
| HF/aug-QZVPPP                       | 3.122/3.112                         | 149.0/178.3 |   | not bound |      | 3.020/3.821                        | 176.9/145.7                              | -0.45 | 0.04 |
| B3LYP/aug-QZVPPP                    | 3.095/3.047                         | 158.0/168.6 |   | not bound |      | 2.707/3.526                        | 178.0/143.2                              | -0.42 | 0.05 |
| MP2/aug-QZVPPP                      | 2.808/2.891                         | 111.9/147.2 |   | -1.67     | 0.37 | 2.612/2.583                        | 145.2/99.6                               | -3.99 | 0.66 |

(B3LYP), 1–9% (HF). For the methane dimer (**1**), for which several theoretical studies have been performed,<sup>[38]</sup> the intermolecular attraction is entirely dominated by dispersion. Independently of the basis set used, **1a** and **1b** are not bound at the HF and B3LYP levels (Figure 1). For the smallest basis set, the BEs with these methods are negative; however, after correction for BSSE the resulting CPBEs adopt positive values, (Table 2 and Table 3). For larger basis sets, however, the calculated BEs are also positive, which demonstrates the inability of both methods to describe the dispersion interactions. These values are not presented in Table 2

and Table 3 because they are not physically meaningful. Despite its longer H–H distances, **1b** is more stable than **1a**. From Figure 1 it is evident that the greater stability of **1b** can be entirely attributed to the increase of dispersion contributions. The MP2/aug-QZVPPP counterpoise-corrected binding energy of **1b** ( $-1.30 \text{ kJ mol}^{-1}$ ) approaches the experimental estimates based on spherically averaged potentials ( $-1.38$  to  $-1.92 \text{ kJ mol}^{-1}$ ).<sup>[39]</sup> It should be noted, however, that **1b** is not the most stable conformer of the methane dimer<sup>[38]</sup> even though the energy differences are small. Figure 1 clearly shows that electrostatic interactions are not

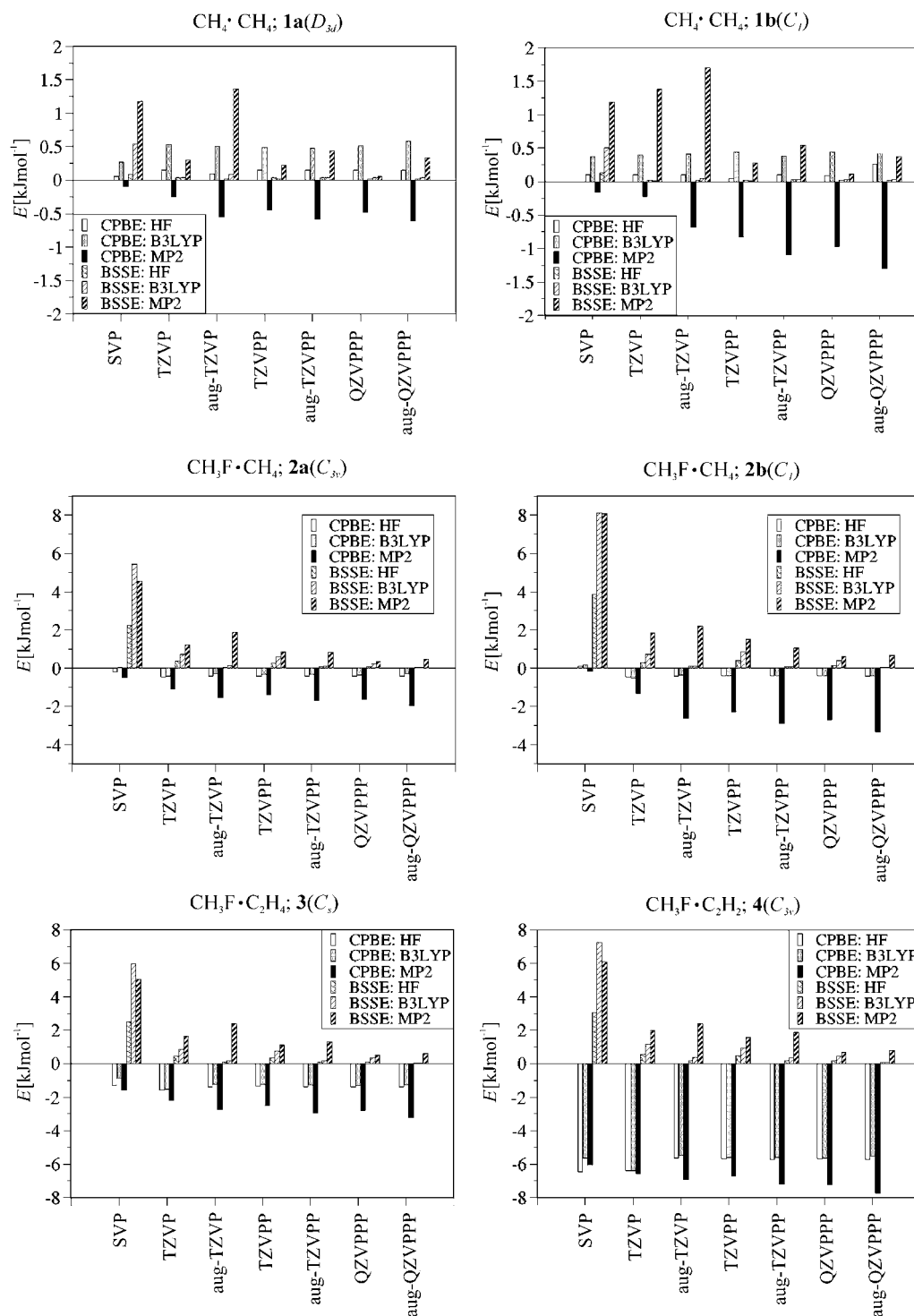


Figure 1. Counterpoise-corrected binding energies (CPBE) and BSSE of **1–4**. For the indicated basis set the ordering is CPBE(HF, B3LYP, MP2) and BSSE(HF, B3LYP, MP2).

discernible in **1a** and **1b**, but they begin to develop for **2a** and **2b**. At the MP2/QZVPPP level, the electrostatic contribution to the whole attraction is 27% for **2a** and 15% for **2b**. Similar to the case of the methane dimer, **2b** is more stable than **2a**, and its greater stability also results from the increased dispersion contribution (see Figure 1). For **3** and **4**, the electrostatic part of the CPBE increases to 49% and 78%, respectively; in the latter case it reaches the value typ-

ically found for conventional hydrogen bridges.<sup>[2a,29]</sup> There are no experimental estimates of the binding energies of **2–4**. Our MP2/QZVPPP studies predict  $-1.62 \text{ kJ mol}^{-1}$  for **2a**,  $-2.72 \text{ kJ mol}^{-1}$  for **2b**,  $-2.79 \text{ kJ mol}^{-1}$  for **3**, and  $-7.25 \text{ kJ mol}^{-1}$  for **4**.

Similar trends are also observed with the other basis sets (Table 2, Table 3, Figure 1). These results clearly show that similar CPBE values, as in the case of **2b** ( $-2.72 \text{ kJ mol}^{-1}$ )

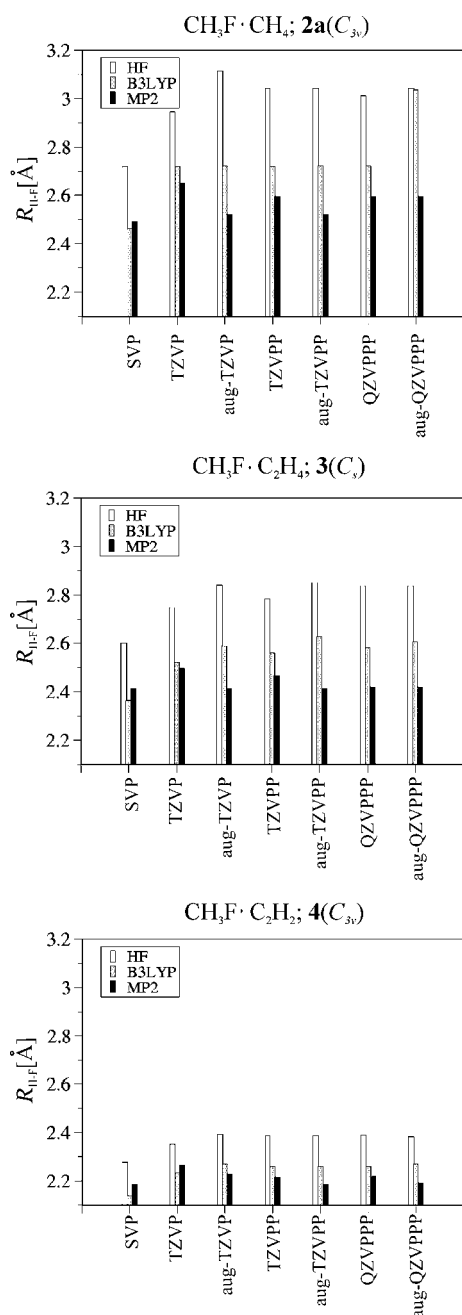


Figure 2. Comparison of the optimized H...F distances of **2a**, **3**, and **4** as a function of the basis set and method.

and **3** ( $-2.79$  kJ mol $^{-1}$ ), do not necessarily indicate a comparable nature or type of hydrogen bridging. To the best of our knowledge, theoretical studies on **2b**, **3**, and **4** are not known, and only one study has appeared for **2a**.<sup>[17a]</sup> On the basis of MP2 calculations with a TZV++(3d1f,1p) basis set augmented with an (1p1d1f)-expansion midway between the F and H atoms, Howard et al. estimated a very short F...H distance of  $\sim 2.2$  Å and an interaction energy of  $-0.85$  kJ mol $^{-1}$ .<sup>[17a]</sup> The basis set used for the hydrogen atoms had only a single p-polarization function and a single diffuse s-shell.<sup>[17a]</sup> We suppose that the calculated interaction energy ( $-0.85$  kJ mol $^{-1}$ ) suffers from a large BSSE, which

normally occurs when basis sets that are not well balanced are used in calculations. In addition, the bond functions used might be problematic.<sup>[40]</sup> Our MP2/aug-TZVPP calculation predicts an interaction energy of  $-1.70$  kJ mol $^{-1}$  for **2a** and  $-2.91$  kJ mol $^{-1}$  for **2b**, and the binding increases at the MP2/aug-QZVPPP level as  $-1.96$  kJ mol $^{-1}$  (**2a**) and  $-3.33$  kJ mol $^{-1}$  (**2b**). Despite these larger interaction energies, the MP2/aug-QZVPPP-optimized F...H distances [ $2.596$  Å (**2a**),  $2.612$  Å (**2b**)], though slightly shorter than the sum of the van der Waals radii, are significantly longer than that determined by Howard et al. ( $2.2$  Å).<sup>[17a]</sup> It is interesting to note that the MP2/aug-QZVPPP attraction of **2a** ( $-1.96$  kJ mol $^{-1}$ ) is only slightly lower than that determined by Caminati and co-workers for a unique C–H...F–C interaction in the difluoromethane dimer ( $-2.2$  kJ mol $^{-1}$ ) by means of free-jet millimeter-wave absorption spectroscopy experiments.<sup>[41]</sup>

Independently of the basis set and calculation method, the optimized F...H distance of **2b** is always longer than that of **2a**. Taking into account that **2b** may be regarded as a bifurcated hydrogen bridging system, this elongation is not surprising. Furthermore, for the more flexible basis sets, the MP2-optimized H–H1 distance of **2b** is significantly shorter than the H–H1 and H–H2 distances in the methane dimer **1b** (Table 3).

The replacement of the C(sp $^3$ )–H donor bond by a C(sp $^2$ )–H and further by a C(sp)–H bond leads to very short F...H contacts (Table 2, Figure 2). The MP2-optimized F...H distances range from  $2.415$  Å to  $2.496$  Å for **3** and from  $2.186$  Å to  $2.266$  Å for **4**. Experimental structures are not available for **3** and **4**. However, we can compare our data with X-ray crystallography measurements of the closely related fluorobenzenes and the 4-ethynylfluorobenzene.<sup>[11a,b]</sup> The MP2/aug-QZVPPP-optimized F...H contacts in **3** ( $2.419$  Å) and **4** ( $2.193$  Å) are only slightly shorter than the experimental values of monofluorinated benzene ( $2.47$  Å)<sup>[11b]</sup> and 4-ethynylfluorobenzene ( $2.26$  Å).<sup>[11a]</sup> This discrepancy may be attributed to the slightly poorer acceptor ability of the C(sp $^2$ )–F bonds<sup>[17a]</sup> present in the “real” molecules compared to the corresponding C(sp $^3$ )–F bonds used in our model systems. The bifurcated nature of the hydrogen bridges in the experimentally investigated monofluorinated benzenes<sup>[11b]</sup> may also be responsible for slightly longer F...H bonds.

Compared to free acetylene, the C–H proton donor bond of **4** is elongated by  $0.0023$  Å (B3LYP/QZVPPP) or  $0.0022$  Å (MP2/QZVPPP). In complex **4**, both C–H stretching modes of the acetylene are red shifted:  $\Delta\nu = -11$  cm $^{-1}$  and  $-4$  cm $^{-1}$  (B3LYP);  $-12$  cm $^{-1}$  and  $-8$  cm $^{-1}$  (MP2). At the MP2/QZVPPP level, we do not observe significant changes in the proton donor C–H bond lengths of **2a** and **3**; however, the remaining C–H bonds are slightly elongated ( $0.0003$ – $0.0005$  Å) compared to those of CH $_4$  and C $_2$ H $_4$ . The shifts of the C–H stretching vibrations are insignificant for complex **3** ( $\Delta\nu = +1$ – $-1$  cm $^{-1}$ ), but in the case of **2a** one C–H stretching mode is blue-shifted ( $\Delta\nu = +4$  cm $^{-1}$ ) while the three other are red-shifted ( $\Delta\nu = -4$  cm $^{-1}$ ,  $-4$  cm $^{-1}$ ,  $-2$  cm $^{-1}$ ). Similar results were also obtained at the B3LYP/QZVPPP level.

To verify to which extent the MP2 method accounts for correlation effects, we have performed QCISD and QCISD(T) calculations for **1–4** with the TZVPP basis and the MP2/TZVPP structures. The CPBEs are presented in Table 4.

Table 4. MP2, QCISD, and QCISD(T) counterpoise-corrected binding energies (CPBE) of **1–4**. The CPBEs [kJ mol<sup>-1</sup>] refer to the TZVPP basis set and MP2/TZVPP structures.

|   | QCISD | MP2   | QCISD(T) |
|---|-------|-------|----------|
| CH <sub>3</sub> :CH <sub>4</sub> , <b>1a</b> (D <sub>3d</sub> )               | -0.39 | -0.45 | -0.56    |
| CH <sub>2</sub> :CH <sub>4</sub> , <b>1b</b> (C <sub>1</sub> )                | -0.65 | -0.83 | -0.92    |
| CH <sub>3</sub> F:CH <sub>4</sub> , <b>2a</b> (C <sub>3v</sub> )              | -1.21 | -1.39 | -1.45    |
| CH <sub>3</sub> F:CH <sub>4</sub> , <b>2b</b> (C <sub>1</sub> )               | -1.91 | -2.31 | -2.42    |
| CH <sub>3</sub> F:C <sub>2</sub> H <sub>4</sub> , <b>3</b> (C <sub>s</sub> )  | -2.30 | -2.50 | -2.60    |
| CH <sub>3</sub> F:C <sub>2</sub> H <sub>2</sub> , <b>4</b> (C <sub>3v</sub> ) | -6.51 | -6.71 | -6.80    |

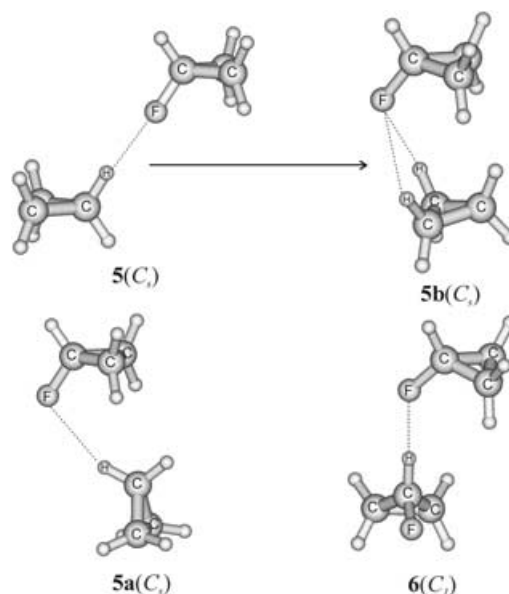
The QCISD(T) CPBEs are larger than the MP2 ones by 0.11 kJ mol<sup>-1</sup> (**1a**), 0.06 kJ mol<sup>-1</sup> (**2a**), 0.10 kJ mol<sup>-1</sup> (**3**), and 0.09 kJ mol<sup>-1</sup> (**4**). These results clearly show that MP2 accounts fairly accurately for the dispersion interactions. The QCISD binding energies are slightly underestimated compared to QCISD(T) ones indicating the importance of triples contributions for the systems studied.

To study the basis set convergence of the correlation energy we have used the common two-point approximation<sup>[56]</sup> with two consecutive cardinal numbers X of the aug-cc-pVXZ (X = 3, 4) basis set.<sup>[55]</sup> The extrapolated aug-cc-pV(TQ)Z BEs are: -2.04 kJ mol<sup>-1</sup> (**2a**), -3.74 kJ mol<sup>-1</sup> (**3**), -8.55 kJ mol<sup>-1</sup> (**4**). Compared to the MP2/aug-cc-pVQZ or MP2/aug-QZVPPP results, the extrapolated values differ by no more than 0.40 kJ mol<sup>-1</sup>. The extrapolated aug-cc-pV(TQ)Z CPBEs of -1.85 kJ mol<sup>-1</sup> (**2a**), -3.38 kJ mol<sup>-1</sup> (**3**), -7.97 kJ mol<sup>-1</sup> (**4**) are within 0.24 kJ mol<sup>-1</sup> of the aug-cc-pVQZ or the aug-QZVPPP values.

### C–H...F–C interactions in monofluorinated cyclopropanes:

To obtain some insight into the nature of the C–H...F–C in-

teractions in the experimentally characterized monofluorinated phenylcyclopropanes,<sup>[11d]</sup> we carried out calculations for the model systems C<sub>3</sub>H<sub>6</sub>:C<sub>3</sub>H<sub>5</sub>F (**5**) and C<sub>3</sub>H<sub>5</sub>F:C<sub>3</sub>H<sub>5</sub>F (**6**) (Scheme 2).



Scheme 2. Molecular structures of the complexes **5a**, **5b**, and **6**.

The calculations for **5** were performed within C<sub>s</sub> symmetry constraints. During the geometry optimization, the starting structure, **5**(C<sub>s</sub>) converged to the bifurcated structure **5b**(C<sub>s</sub>) which, in addition, has relatively short ring–ring contacts. Further searches on the potential energy surface leads to structure **5a**(C<sub>s</sub>) with only one C–H...F contact. The geometry optimization for **6** was carried out without any symmetry constraints. The calculated data are summarized in Table 5 and graphically displayed in Figure 3, Figure 4, and Figure 5.

As expected, the calculated BSSEs decrease systematically as the basis set is improved. The BEs and CPBEs con-

Table 5. Optimized H–F bond lengths [Å] and C–H–F bond angles [°] as well as calculated binding energies (BE) [kJ mol<sup>-1</sup>] and basis set superposition errors (BSSE) [kJ mol<sup>-1</sup>] for the conformers **5a** and **5b** of the C<sub>3</sub>H<sub>5</sub>F:C<sub>3</sub>H<sub>6</sub> system and for C<sub>3</sub>H<sub>5</sub>F:C<sub>3</sub>H<sub>5</sub>F (**6**).

| Method/basis    | <b>5b</b> (C <sub>s</sub> ) |       |        |       | <b>5a</b> (C <sub>s</sub> ) |       |        |      | <b>6</b> (C <sub>s</sub> ) |       |        |      |
|-----------------|-----------------------------|-------|--------|-------|-----------------------------|-------|--------|------|----------------------------|-------|--------|------|
|                 | R <sub>H–F</sub>            | ∠CHF  | BE     | BSSE  | R <sub>H–F</sub>            | ∠CHF  | BE     | BSSE | R <sub>H–F</sub>           | ∠CHF  | BE     | BSSE |
| HF/SVP          | 2.873                       | 116.7 | -4.88  | 4.49  | 2.701                       | 180.0 | -3.88  | 3.40 | 2.587                      | 161.3 | -5.82  | 3.29 |
| B3LYPSVP        | 2.625                       | 118.8 | -8.76  | 9.76  | 2.508                       | 169.0 | -6.80  | 6.82 | 2.410                      | 179.9 | -8.63  | 6.99 |
| MP2/SVP         | 2.573                       | 117.3 | -13.57 | 11.62 | 2.476                       | 168.5 | -10.87 | 8.56 | 2.392                      | 178.1 | -11.19 | 8.29 |
| HF/TZVP         | 3.098                       | 120.5 | -1.96  | 0.72  | 2.905                       | 174.6 | -1.40  | 0.50 | 2.735                      | 123.2 | -4.66  | 0.90 |
| B3LYP/TZVP      | 3.234                       | 122.4 | -1.08  | 1.00  | 2.793                       | 166.9 | -1.31  | 0.73 | 2.559                      | 176.7 | -3.37  | 0.92 |
| MP2/TZVP        | 2.695                       | 120.3 | -9.33  | 4.45  | 2.494                       | 161.0 | -7.52  | 4.14 | 2.463                      | 175.7 | -7.19  | 3.13 |
| HF/aug-TZVP     | 3.104                       | 119.9 | -1.51  | 0.34  | 2.965                       | 175.6 | -1.07  | 0.23 | 2.920                      | 117.1 | -4.29  | 0.47 |
| B3LYP/aug-TZVP  | 3.018                       | 123.9 | -0.70  | 0.31  | 2.814                       | 170.1 | -0.77  | 0.22 | 2.626                      | 176.6 | -2.86  | 0.28 |
| MP2/aug-TZVP    | 2.632                       | 120.0 | -13.39 | 6.03  | 2.493                       | 159.5 | -11.79 | 6.52 | 2.618                      | 116.6 | -17.37 | 8.07 |
| HF/TZVPP        | 2.875                       | 117.2 | -1.18  | 0.74  | 3.014                       | 144.5 | -1.39  | 0.41 | 2.861                      | 122.1 | -4.35  | 0.66 |
| B3LYP/TZVPP     | 3.375                       | 127.0 | -0.55  | 0.78  | 2.850                       | 168.8 | -1.17  | 0.67 | 2.786                      | 123.7 | -4.26  | 1.23 |
| MP2/TZVPP       | 2.702                       | 124.8 | -9.68  | 2.57  | 2.484                       | 160.3 | -7.16  | 2.04 | 2.571                      | 117.4 | -11.91 | 3.00 |
| HF/aug-TZVPP    | 3.724                       | 117.3 | -0.47  | 0.10  | 2.977                       | 179.7 | -0.94  | 0.12 | 2.884                      | 122.4 | -3.88  | 0.19 |
| B3LYP/aug-TZVPP | 3.613                       | 127.6 | 0.08   | 0.12  | 2.845                       | 166.2 | -0.63  | 0.17 | 2.562                      | 176.6 | -2.77  | 0.23 |
| MP2/aug-TZVPP   | 2.680                       | 124.7 | -11.00 | 2.86  | 2.580                       | 157.0 | -8.68  | 2.54 | 2.559                      | 115.3 | -13.83 | 2.82 |
| HF/QZVPPP       | 2.876                       | 117.3 | -0.76  | 0.29  | 3.014                       | 144.1 | -1.18  | 0.18 | 2.861                      | 122.1 | -3.95  | 0.27 |
| B3LYP/QZVPPP    | 3.365                       | 126.9 | -0.03  | 0.28  | 2.850                       | 168.8 | -0.74  | 0.23 | 2.786                      | 123.7 | -3.57  | 0.47 |
| MP2/QZVPPP      | 2.712                       | 124.9 | -8.79  | 0.99  | 2.605                       | 155.3 | -6.78  | 0.81 | 2.574                      | 117.1 | -11.30 | 1.28 |

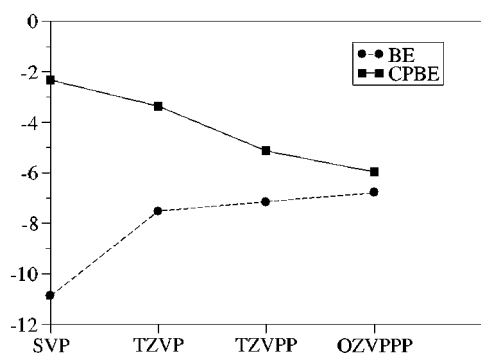


Figure 3. The MP2 interaction energy of **5a** (in  $\text{kJ mol}^{-1}$ ) as a function of the basis set. The dashed line is the uncorrected BE curve and the solid line is the counterpoise-corrected CPBE curve.

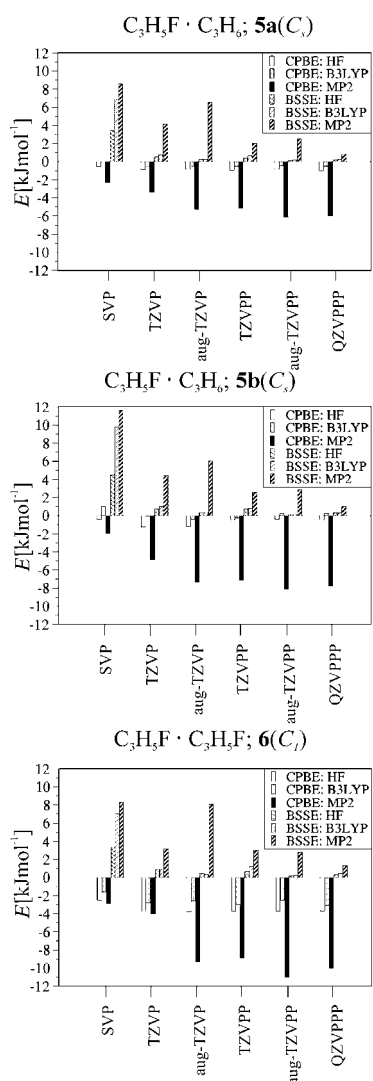


Figure 4. Counterpoise-corrected binding energies (CPBE) and BSSE of **5a**, **5b**, and **6**. For the indicated basis set the ordering is CPBE(HF, B3LYP, MP2) and BSSE(HF, B3LYP, MP2).

verge towards the same interaction energy, as shown schematically for **5a** in Figure 3.

With respect to the method used, the optimized F...H distances of **5** and **6** show the same trends as in the case of **2**–

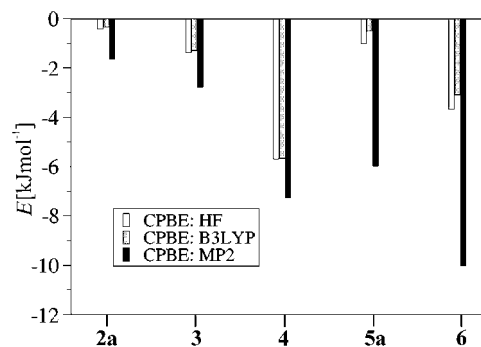


Figure 5. Counterpoise-corrected binding energies CPBE(HF, B3LYP, MP2) of **2a**, **3**, **4**, **5a**, and **6** calculated with the QZVPPP basis set.

**4**:  $R_{\text{F-H}}(\text{HF}) > R_{\text{F-H}}(\text{B3LYP}) > R_{\text{F-H}}(\text{MP2})$  (Table 5). For a given basis set, similarly to the case of **1**–**4**, the absolute BSSEs are larger at the correlated MP2 than at HF and B3LYP levels (see Figure 1 and Figure 4).

Contrary to what is found at the HF level, **5b** is not bound at the B3LYP level. The PBE/TZVPP method predicts a CPBE of  $-2.92 \text{ kJ mol}^{-1}$  for **5b**, which is, however, underestimated compared to the corresponding MP2/TZVPP value ( $-7.11 \text{ kJ mol}^{-1}$ ). On the other hand, a comparative DFT study on hydrogen-bonded systems showed that the PBE functional normally overestimates binding energies compared to MP2.<sup>[42]</sup> The MP2/QZVPPP F...H distance of **5a** ( $2.605 \text{ \AA}$ ) is of the same magnitude as that of **2a** ( $2.596 \text{ \AA}$ ), and the F...H distance of **6** ( $2.574 \text{ \AA}$ ) is only slightly shorter (Table 5).

The F...H distances (MP2) of the bifurcated structure **5b** are always longer than that in **5a**, and, with the more extended basis set, even longer than the sum of the van der Waals radii. Once again, despite the long F...H contacts, the bifurcated structure **5b** is more stable than **5a**. At the MP2/QZVPPP level of theory, the counterpoise-corrected interaction energy (CPBE) amounts to  $-7.80 \text{ kJ mol}^{-1}$  for **5b** and  $-5.97 \text{ kJ mol}^{-1}$  for **5a** (Figure 4). Figure 4 clearly shows that for both, **5a** and **5b**, dispersion is the dominant term of the entire attraction. Electrostatic contributions are also present, but they are small [17% (**5a**), 6% (**5b**)]. For **6** the MP2/QZVPPP counterpoise-corrected binding energy is  $-10.02 \text{ kJ mol}^{-1}$ , which is of the same magnitude as that of the fluoromethane–water complex ( $-9.95 \text{ kJ mol}^{-1}$ )<sup>[17a]</sup> and even larger than for the fluoromethane–acetylene complex, **4** ( $-7.25 \text{ kJ mol}^{-1}$ ). Similar energies were also obtained for the difluoromethane–water complex from CCSD(T)/6-311 + G(d) ( $-9.91 \text{ kJ mol}^{-1}$ ) and experimental ( $-7.5 \text{ kJ mol}^{-1}$ ) studies.<sup>[9]</sup> The electrostatic contribution to the CPBE of **6** amounts to 37% (MP2/QZVPPP).

Compared to the monomer, the C–H proton-donor bond of **6** is shortened by  $0.0008 \text{ \AA}$  (B3LYP/QZVPPP) or  $0.0010 \text{ \AA}$  (MP2/QZVPPP). The corresponding C–H stretching mode is blue-shifted,  $\Delta\nu = +15 \text{ cm}^{-1}$ .

In Figure 5, we compare the counterpoise-corrected binding energies of **2a**, **3**, **4**, **5a**, and **6** calculated at the HF, B3LYP, and MP2 levels with the QZVPPP basis set.

It can be seen that the MP2 interaction energy increases in the order  $2\mathbf{a} < \mathbf{3} < \mathbf{5a} < \mathbf{4} < \mathbf{6}$ , while for HF and B3LYP the



ordering is:  $2\mathbf{a} < 5\mathbf{a} < 3 < 6 < 4$  (Figure 5). The HF and B3LYP CPBEs, which only contain electrostatic contributions, suggest that the proton-donating ability of the C–H bond in  $\mathbf{6}$  may be classified as between that of the  $C(sp^2)$ –H bond of  $\mathbf{3}$  and the  $C(sp)$ –H bond of  $\mathbf{4}$ . This finding is in perfect agreement with early experimental and theoretical studies on the acidity of the different kinds of C–H bonds.<sup>[7d,e,43]</sup> It should be noted, however, as a result of the unconstrained geometry optimizations in  $\mathbf{6}$ , the fluorine atom is attached to the same carbon atom as the interacting proton (Scheme 2). Consequently, the donating bond in  $\mathbf{6}$  should be more correctly classified as an activated C–H donor. Although such situations are not possible for the experimentally characterized 2-fluoro-2-phenylcyclopropane derivatives,<sup>[11d]</sup> the question whether other substituents in the

three-membered ring may influence the acidity and the basicity of the cyclopropane C–H and C–F bonds requires further systematic studies.

**Potential energy curves (PEC) of 2–4:** In this section we wish to discuss the problem concerning the effect of the BSSE on the optimized H...F distances. On the left-hand side of Figure 6 we show the calculated potential energy curves (PEC) obtained by varying the H...F distance. The counterpoise-corrected PECs are shown on the right-hand side of Figure 6. Independent of the method employed, the counterpoise-corrected H...F distances ( $R_{H-F}^{CP}$ ) are always longer than the corresponding uncorrected values ( $R_{H-F}$ ). This finding is in agreement with literature data;<sup>[44]</sup> however, the lengthening of  $R_{H-F}^{CP}$  is rather large in the case of the

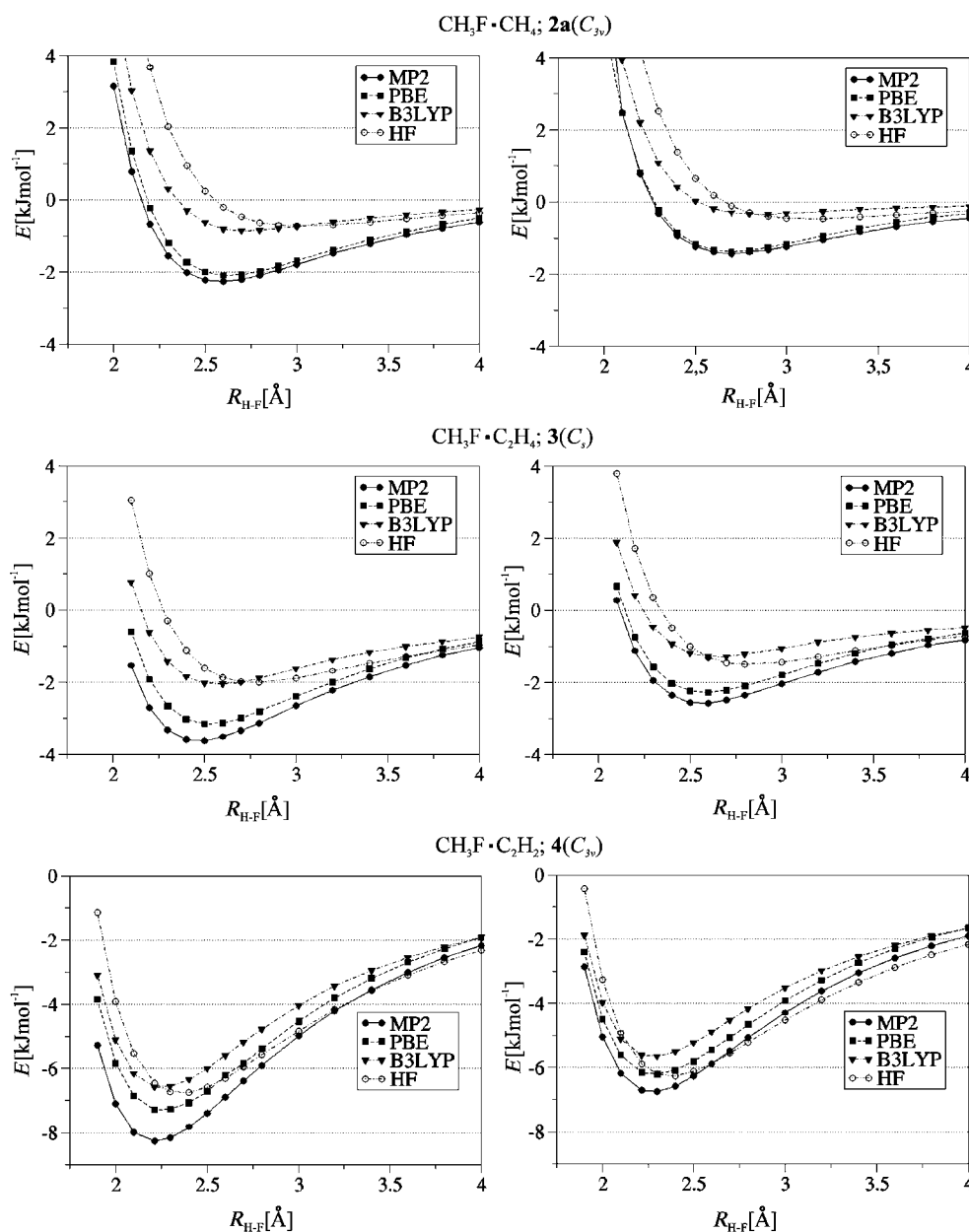


Figure 6. Uncorrected (left-hand side) and BSSE-corrected (right-hand side) interaction energies of  $2\mathbf{a}$ ,  $\mathbf{3}$ , and  $\mathbf{4}$  as a function of the intramolecular separation,  $R_{H-F}$ , calculated with the TZVPP basis set.

systems dominated by dispersion interactions [for example, **2a**: 0.102 Å (MP2), 0.082 Å (PBE), 0.118 Å (B3LYP), 0.130 Å (HF)]. For CH<sub>3</sub>F·C<sub>2</sub>H<sub>2</sub> (**4**), where electrostatic contributions determine the nature of the C–H···F–C bonding,  $R_{\text{H-F}}$  and  $R_{\text{H-F}}^{\text{CP}}$  are closer together and the elongation [0.056 Å (MP2), 0.032 Å (PBE), 0.026 Å (B3LYP), 0.015 Å (HF)] is of the same order as that found for conventional hydrogen bonding.<sup>[45]</sup>

For CH<sub>3</sub>F·C<sub>2</sub>H<sub>4</sub> (**3**), the elongation due to the CP correction lies between that of **2a** and **4** [0.078 Å (MP2), 0.062 Å (PBE), 0.103 Å (B3LYP), 0.049 Å (HF)]. Based on these results, it can be concluded that, in addition to the calculated BE values, the structural parameters of dispersion-dominated systems are more affected by BSSE compared to conventional hydrogen bridges and, consequently, these systems are more demanding with respect to the theoretical method and the quality of the basis set. Considering the shapes of the PECs in Figure 6, the following conclusions can be drawn: the counterpoise-corrected curves are closer together than the uncorrected ones. For dispersion-dominated bonding, the PECs are shallow and wide. In agreement with the fact, that the hybrid B3LYP functional is not able to account for dispersion forces, these curves are close to the HF ones, but a crossing is observed at longer H···F distances. The DFT/PBE curves are very close and parallel to the MP2 ones.

## Conclusion

We investigated the nature and the strength of C–H···F–C interactions with hierarchies of basis sets and ab initio [HF, MP2, QCISD, QCISD(T)] and density functional theory (DFT/B3LYP and DFT/PBE) methods for the C(sp<sup>3</sup>)–H, C(sp<sup>2</sup>)–H, and C(sp)–H donors and F–C(sp<sup>3</sup>) acceptors. Basis sets of double-zeta quality are not appropriate for the investigation of these weakly bonded systems. To obtain conclusive results, well-balanced basis sets of at least TZVPP quality are needed. The optimized F···H distances follow the order:  $R_{\text{H-F}}(\text{HF}) > R_{\text{H-F}}(\text{B3LYP}) > R_{\text{H-F}}(\text{MP2})$ . In **2**, **3**, **5**, and **6**, the dispersion interaction is the dominant term of the entire attraction. Depending on the dispersion contribution to the bonding, the CP-corrected MP2/TZVPP distances are stretched by 0.06–0.1 Å with respect to the uncorrected ones. The MP2/QZVPPP  $R_{\text{H-F}}$  distances of **2a** (2.596 Å), **5a** (2.605 Å), and **6** (2.574 Å), though slightly shorter than the sum of the van der Waals radii, are significantly longer than the threshold (2.3 Å) used in CSD studies.<sup>[17]</sup> The bifurcated structures **1b**, **2b**, and **5b**, despite longer H···F/H distances than in **1a**, **2a**, and **5a**, are characterized by stronger bonding owing due to the increased dispersion interactions. The replacement of the C(sp<sup>3</sup>)–H donor bond by a C(sp<sup>2</sup>)–H and further by a C(sp)–H bond results in significantly shortened F···H contacts, namely, 2.418 Å (**3**), 2.218 Å (**4**), which agree well with the experimental values determined for the related monofluorinated benzenes (2.47 Å) and 4-ethynylfluorobenzenes (2.26 Å).<sup>[11]</sup> The MP2/aug-QZVPPP interaction energy of **2a** (–1.96 kJ mol<sup>–1</sup>) is close to that determined experimentally

for a unique C–H···F–C interaction in the difluoromethane dimer (–2.2 kJ mol<sup>–1</sup>).<sup>[41]</sup> The calculated interaction energy of **6** (–10.02 kJ mol<sup>–1</sup>) is of the same magnitude as that of the fluoromethane–water complex (–9.95 kJ mol<sup>–1</sup>)<sup>[17a]</sup> and even greater than that of the fluoromethane–acetylene complex **4** (–7.25 kJ mol<sup>–1</sup>). These values can be compared with the CCSD(T)/6-311G+(d) result (–9.91 kJ mol<sup>–1</sup>) or with the experimental value (–7.5 kJ mol<sup>–1</sup>) for the difluoromethane–water complex.<sup>[9]</sup> The effects of electron correlation beyond MP2 are small; the QCISD(T) CPBEs of **1–4** are lower in energy than the MP2 ones by only 0.06–0.11 kJ mol<sup>–1</sup>. Significant electrostatic interactions are observed for **6** and **3**. In **4**, these forces dominantly contribute to the hydrogen bonding. The C(sp)–H···F–C(sp<sup>3</sup>) interaction in **4**, though weak, shows the same characteristics as conventional hydrogen bridges. The proton-donating ability of the C–H bond of **6** can be classified as being between that of the C(sp<sup>2</sup>)–H bond of **3** and the C(sp)–H bond of **4**. The comparable absolute values of the bond strengths do not necessarily indicate a comparable nature or type of the hydrogen bridges. For dispersion-dominated systems, contrary to the hybrid DFT/B3LYP method, pure DFT/PBE provides results which are close to the MP2 ones.

## Acknowledgment

This work was supported by the Deutsche Forschungsgemeinschaft in the framework of the SFB424 (“Molekulare Orientierung als Funktionskriterium in chemischen Systemen”). We thank Dr. C. Mück-Lichtenfeld for technical support and helpful discussions.

- [1] a) L. Pauling, *The Nature of the Chemical Bond*, Cornell University Press, Ithaca, NY, 1960; b) G. C. Pimentel, A. L. McClellan, *The Hydrogen Bond*, Freeman, San Francisco, CA, 1960.
- [2] a) G. R. Desiraju, T. Steiner, *The Weak Hydrogen Bond in Structural Chemistry and Biology*, IUCR Monographs on Crystallography, Vol. 9, Oxford University Press, Oxford 1999; b) G. A. Jeffrey, W. Saenger, *Hydrogen Bonding in Biological Structures*, Springer-Verlag, Berlin, Heidelberg, 1994; c) G. R. Desiraju, *Acc. Chem. Res.* **2002**, *35*, 565–573.
- [3] R. M. Badger, S. H. Bauer, *J. Chem. Phys.* **1937**, *5*, 839–851.
- [4] a) R. Gerald, T. Bernhard, U. Haeberlen, J. Rendell, S. Opella, *J. Am. Chem. Soc.* **1993**, *115*, 777–782; b) A. Ramamoorthy, C. H. Wu, S. Opella, *J. Am. Chem. Soc.* **1997**, *119*, 10479–10486; c) M. Pham, M. Gdaniec, T. Połoński, *J. Org. Chem.* **1998**, *63*, 3731–3734; d) J. E. Del Bene, S. A. Perera, R. J. Barlett, *J. Phys. Chem. A.* **1999**, *103*, 8121–8124; e) A. Bagno, G. Saielli, G. Scorrano, *Chem. Eur. J.* **2002**, *8*, 2047–2056.
- [5] a) S. A. Harrell, D. H. McDaniel, *J. Am. Chem. Soc.* **1964**, *86*, 4497–4497; b) J. W. Larson, T. B. McMahon, *J. Am. Chem. Soc.* **1983**, *105*, 2944–2950; c) J. W. Larson, T. B. McMahon, *J. Am. Chem. Soc.* **1984**, *106*, 517–521; d) P. Gilli, V. Ferretti, V. Bertolasi, G. Gilli, *J. Am. Chem. Soc.* **1994**, *116*, 909–915; e) P. Gilli, V. Bertolasi, V. Ferretti, G. Gilli, *J. Am. Chem. Soc.* **2000**, *122*, 10405–10417.
- [6] M. Calhorda, *Chem. Commun.* **2000**, 801–809.
- [7] a) S. Glasstone, *Trans. Faraday Soc.* **1937**, *33*, 200–214; b) R. D. Green, *Hydrogen Bonding by C-H Groups*, McMillan, London, **1974**; c) D. J. Sutor, *Nature* **1962**, *195*, 68–69; d) A. Allerhand, P. von R. Schleyer, *J. Am. Chem. Soc.* **1963**, *85*, 1715–1723; e) R. Taylor, O. Kennard, *J. Am. Chem. Soc.* **1982**, *104*, 5063–5070; f) P. Murray-Rust, J. P. Glusker, *J. Am. Chem. Soc.* **1984**, *106*, 1018–1025; g) R. O. Gould, A. M. Gray, P. Taylor, M. D. Walkinshaw, *J. Am. Chem. Soc.* **1985**, *107*, 5921–5927; h) J. A. R. O. Sarma, G. R. Desiraju, *Acc. Chem. Res.* **1986**, *19*, 222–228; i) G. R. Desiraju, *Acc.*

- Chem. Res.* **1991**, *24*, 290–296; j) G. R. Desiraju, *Acc. Chem. Res.* **1996**, *29*, 441–449; k) T. Steiner, *Chem. Commun.* **1997**, 727–734.
- [8] a) J. J. Novoa, B. Tarron, M.-H. Whangbo, J. M. Williams, *J. Chem. Phys.* **1991**, *95*, 5179–5186; b) L. Turi, J. J. Dannenberg, *J. Phys. Chem.* **1993**, *97*, 7899–7909; c) T. Van Mourik, F. B. Duijneveldt, *J. Mol. Struct.* **1995**, *341*, 63–73; d) Y. Gu, T. Kar, S. Scheiner, *J. Am. Chem. Soc.* **1999**, *121*, 9411–9422.
- [9] a) R. West, D. L. Powell, L. S. Whatley, M. K. T. Lee, P. von R. Schleyer, *J. Am. Chem. Soc.* **1962**, *84*, 3221–3222; b) D. A. K. Jones, J. G. Watkinson, *J. Chem. Soc.* **1964**, 2366–2370; c) P. J. Krueger, H. D. Mettee, *Can. J. Chem.* **1964**, *42*, 326–339; d) A. W. Baker, A. T. Shulgin, *Can. J. Chem.* **1965**, *43*, 650–659; e) R. G. Azrak, E. B. Wilson, *J. Chem. Phys.* **1970**, *52*, 5299–5316; f) P. Murray-Rust, W. C. Stallings, C. T. Monti, R. K. Preston, J. P. Glusker, *J. Am. Chem. Soc.* **1983**, *105*, 3206–3214; g) R. J. Abraham, T. A. D. Smith, W. A. Thomas, *J. Chem. Soc. Perkin Trans. 2* **1996**, 1949–1955; h) T. J. Barbarich, C. D. Rithner, S. M. Miller, O. P. Anderson, S. H. Strauss, *J. Am. Chem. Soc.* **1999**, *121*, 4280–4281; i) W. Caminati, S. Melandri, I. Rossi, P. G. Favero, *J. Am. Chem. Soc.* **1999**, *121*, 10098–10101; j) J. P. Snyder, N. S. Chandrakumar, H. Sato, D. C. Lankin, *J. Am. Chem. Soc.* **2000**, *122*, 544–545; k) Y. Tatamitani, B. Liu, J. Shimada, T. Ogata, P. Ottaviano, A. Maris, W. Caminati, J. L. Alonso, *J. Am. Chem. Soc.* **2002**, *124*, 2739–2743.
- [10] a) D. A. Dixon, B. E. Smart, *J. Phys. Chem.* **1991**, *95*, 1609–1612; b) I. D. Rae, J. A. Weigold, R. H. Contreras, R. R. Biekofsky, *Magn. Reson. Chem.* **1993**, *31*, 836–840; c) R. J. Abraham, E. J. Chambers, W. A. Thomas, *J. Chem. Soc. Perkin Trans. 2* **1994**, 949–955; d) J. M. Bakke, L. H. Bjerkeseth, E. C. L. Rønnow, K. Steinsvoll, *J. Mol. Struct.* **1994**, *321*, 205–214; e) M. A. Biamonte, A. Vasella, *Helv. Chim. Acta* **1998**, *81*, 695–717; f) J. W. Banks, A. S. Batsanov, J. A. K. Howard, D. O'Hagan, H. S. Rzepa, S. Martin-Santamaria, *J. Chem. Soc. Perkin Trans. 2* **1999**, 2409–2411; g) E. Clot, O. Eisenstein, R. H. Crabtree, *New J. Chem.* **2001**, *25*, 66–72; h) D. C. Lankin, G. L. Grunewald, F. A. Romero, I. Y. Oren, J. P. Snyder, *Org. Lett.* **2002**, *4*, 3557–3560.
- [11] a) H.-C. Weiss, R. Boese, H. L. Smith, M. M. Haley, *Chem. Commun.* **1997**, 2403–2404; b) V. R. Thalladi, H.-C. Weiss, D. Bläser, R. Boese, A. Nangia, G. R. Desiraju, *J. Am. Chem. Soc.* **1998**, *120*, 8702–8710; c) A. Mele, B. Vergani, F. Viani, S. V. Meille, A. Farina, P. Bravo, *Eur. J. Org. Chem.* **1999**, 187–196; d) G. Haufe, T. C. Rosen, O. G. J. Meyer, R. Fröhlich, K. Rissanen, *J. Fluorine Chem.* **2002**, *114*, 189–198.
- [12] a) H.-C. Weiss, D. Bläser, R. Boese, B. M. Doughan, M. M. Haley, *Chem. Commun.* **1997**, 1703–1704; b) J. M. A. Robison, B. M. Kar-iuki, K. D. M. Harris, D. Philip, *J. Chem. Soc. Perkin Trans. 2* **1998**, 2459–2470; c) D. Philip, J. M. A. Robison, *J. Chem. Soc. Perkin Trans. 2* **1998**, 1643–1650; d) P. Hobza, Z. Havlas, *Chem. Rev.* **2000**, *100*, 4253–4264.
- [13] a) Q. Liu, R. Hoffmann, *J. Am. Chem. Soc.* **1995**, *117*, 10108–10112; b) J. Wessel, J. C. Lee, Jr., E. Peris, G. P. A. Yap, J. B. Fortin, J. S. Ricci, G. Sinni, A. Albinati, T. F. Koetzle, O. Eisenstein, A. L. Rheingold, R. H. Crabtree, *Angew. Chem.* **1995**, *107*, 2711–2713; *Angew. Chem. Int. Ed. Engl.* **1995**, *34*, 2507–2509; c) G. Orłowa, S. Scheiner, T. Kar, *J. Phys. Chem. A* **1999**, *103*, 514–520; d) R. H. Crabtree, P. E. M. Siegbahn, O. Eisenstein, A. L. Rheingold, T. F. Koetzle, *Acc. Chem. Res.* **1996**, *29*, 348–354.
- [14] a) R. F. W. Bader, *Atoms in Molecules*, Oxford University Press, Oxford **1990**; b) U. Koch, P. L. A. Popelier, *J. Phys. Chem.* **1995**, *99*, 9747–9754; c) P. L. A. Popelier, G. Logothetis, *J. Organomet. Chem.* **1998**, *555*, 101–111; d) P. L. A. Popelier, *J. Phys. Chem. A* **1998**, *102*, 1873–1878.
- [15] L. Shimon, J. P. Glusker, *Struct. Chem.* **1994**, *5*, 383–397.
- [16] a) T. J. Welch, S. Eswarakrishnan, *Fluorine in Bioorganic Chemistry*, Wiley, New York, **1991**; b) *Organofluorine Compounds in Medicinal Chemistry and Biomedical Applications* (Eds.: R. Filler, Y. Kobayashi, L. M. Yagupolskii), Elsevier, Amsterdam, **1993**; c) *Enantiocontrolled Synthesis of Fluoro-Organic Compounds. Stereochemical Challenge and Biomedical Targets* (Ed.: V. A. Soloskonok), Wiley, Chichester, **1999**; d) K. L. Kirk, *J. Fluorine Chem.* **1995**, *72*, 261–266; e) D. O'Hagan, H. S. Rzepa, *Chem. Commun.* **1997**, 645–652; f) M. Hoffmann, J. Rychlewski, *J. Am. Chem. Soc.* **2001**, *123*, 2308–2316.
- [17] a) J. A. K. Howard, V. J. Hoy, D. O'Hagan, G. Smith, *Tetrahedron* **1996**, *52*, 12613–12622; b) J. D. Dunitz, R. Taylor, *Chem. Eur. J.* **1997**, *3*, 89–98.
- [18] A. Bondi, *J. Phys. Chem.* **1964**, *68*, 441–451.
- [19] D. J. Teff, J. C. Huffman, K. G. Caulton, *Inorg. Chem.* **1997**, *36*, 4372–4380.
- [20] a) F. A. Cotton, L. M. Daniels, G. T. Jordan, IV, C. A. Murillo, *Chem. Commun.* **1997**, 1673–1674; b) T. A. Evans, K. R. Seddon, *Chem. Commun.* **1997**, 2023–2024; c) M. Mascal, *Chem. Commun.* **1998**, 303–304; d) T. Steiner, G. R. Desiraju, *Chem. Commun.* **1998**, 891–892; M. Schlosser, in ref. [16c], pp. 613–659; International Symposium *Fluorine in the Life Sciences*, Bürgenstock (Switzerland), 6–9 July, **2003**, organized by K.-H. Altmann, P. Maienfisch, K. Müller, M. Schlosser.
- [21] R. Ahlrichs, M. Bär, H.-P. Baron, R. Bauernschmitt, S. Böcker, M. Ehrig, K. Eichkorn, F. Elliot, F. Furche, F. Haase, M. Häser, H. Horn, C. Huber, U. Huniar, M. Kattaneck, C. Kölmel, M. Kollowitz, K. May, C. Ochsenfeld, H. Öhm, A. Schäfer, U. Schneider, O. Treutler, M. von Arnim, F. Weigend, P. Weis, H. Weiss, TURBOMOLE (Vers. 5.3 and 5.5); University of Karlsruhe, Karlsruhe (Germany), **2002**.
- [22] C. Møller, M. S. Plesset, *Phys. Rev.* **1934**, *46*, 618–622.
- [23] A. D. Becke, *J. Chem. Phys.* **1993**, *98*, 5648–5652.
- [24] J. P. Perdew, K. Burke, M. Ernzerhof, *Phys. Rev. Lett.* **1996**, *77*, 3865–3868.
- [25] a) O. Vahtras, J. Almlöf, M. W. Feyereisen, *Chem. Phys. Lett.* **1993**, *213*, 514–518; b) F. Weigend, M. Häser, *Theor. Chem. Acc.* **1997**, *97*, 331–340.
- [26] a) M. O. Sinnokrot, E. F. Valeev, C. D. Sherrill, *J. Am. Chem. Soc.* **2002**, *124*, 10887–10893; b) A. Halkier, H. Koch, P. Jørgensen, O. Christiansen, I. M. Beck Nielsen, T. Helgaker, *Theor. Chem. Acc.* **1997**, *97*, 150–157.
- [27] a) J. A. Pople, M. Head-Gordon, K. Raghavachari, *J. Chem. Phys.* **1987**, *87*, 5968–5975; b) T. Helgaker, P. Jørgensen, J. Olsen, *Molecular Electronic-Structure Theory*, Wiley, Chichester, **2000**.
- [28] S. Grimme, E. Izgorodina, RICC (Version 1.7): A coupled-cluster program that uses the resolution of the identity method. University of Münster, Münster (Germany), **2003**.
- [29] A. K. Rappé, E. R. Bernstein, *J. Phys. Chem. A* **2000**, *104*, 6117–6128.
- [30] S. F. Boys, F. Bernardi, *Mol. Phys.* **1970**, *19*, 553–566.
- [31] a) A. Schäfer, H. Horn, R. Ahlrichs, *J. Chem. Phys.* **1992**, *97*, 2571–2577; b) A. Schäfer, C. Huber, R. Ahlrichs, *J. Chem. Phys.* **1994**, *100*, 5829–5835.
- [32] F. Weigend, M. Häser, H. Patzelt, R. Ahlrichs, *Chem. Phys. Lett.* **1998**, *294*, 143–152.
- [33] a) P. A. Kollman, L. C. Allen, *J. Chem. Phys.* **1970**, *52*, 5085–5094; b) K. Morokuma, *J. Chem. Phys.* **1971**, *55*, 1236–1244; c) H. Umeyama, K. Morokuma, *J. Am. Chem. Soc.* **1977**, *99*, 1316–1332; d) S. L. Price, A. J. Stone, *J. Chem. Phys.* **1987**, *86*, 2859–2868.
- [34] B. Jeziorski, K. Szalewicz, "Intramolecular Interactions by Perturbation Theory", in *Encyclopedia of Computational Chemistry*, Vol. 2, pp. 1376–1398, and references therein, (Eds.: P. von R. Schleyer, N. L. Allinger, T. Clark, J. Gasteiger, P. A. Kollman, H. F. Schaefer, -III, P. R. Schreiner), Wiley, Chichester, UK, **1998**.
- [35] a) T. H. Dunning, *J. Chem. Phys.* **1989**, *90*, 1007–1023; b) R. A. Kendall, T. H. Dunning, R. J. Harrison, *J. Chem. Phys.* **1992**, *96*, 6796–6806; c) D. E. Woon, T. H. Dunning, *J. Chem. Phys.* **1993**, *98*, 1358–1371; d) D. E. Woon, T. H. Dunning, *J. Chem. Phys.* **1994**, *100*, 2975–2988.
- [36] a) T. Helgaker, W. Klopper, H. Koch, J. Noga, *J. Chem. Phys.* **1997**, *106*, 9639–9646; b) A. Halkier, T. Helgaker, P. Jørgensen, W. Klopper, H. Koch, J. Olsen, A. K. Wilson, *Chem. Phys. Lett.* **1998**, *286*, 243–252.
- [37] O. Kind, M. Reiher, J. Neugebauer, B. A. Hess, SNF (Version 2.2.1), Program Package for Numerical Frequency Analyses, University of Erlangen, Erlangen (Germany), **2002**.
- [38] a) J. J. Novoa, M.-H. Whangbo, J. M. Williams, *J. Chem. Phys.* **1991**, *94*, 4835–4841; b) J. Nagy, D. F. Weaver, V. H. Smith, Jr., *Mol. Phys.* **1995**, *85*, 1179–1192; c) S. Tsuzuki, T. Uchimaru, K. Tanabe, *Chem. Phys. Lett.* **1998**, *287*, 202–208; d) R. L. Rowley, T. Pakkanen, *J. Chem. Phys.* **1999**, *110*, 3368–3377.

- [39] a) G. P. Matthews, E. B. Smith, *Mol. Phys.* **1976**, *32*, 1719–1729; b) J. Hoinkis, R. Ahlrichs, H. Böhm, *Int. J. Quantum Chem.* **1983**, *23*, 821–834; c) B. P. Reid, M. J. O'Loughlin, R. K. Sparks, *J. Chem. Phys.* **1985**, *83*, 5656–5662; d) R. Maple, M.-J. Hwang, T. P. Stockfish, U. Dinur, M. Waldman, C. S. Ewig, A. T. Hagler, *J. Comput. Chem.* **1994**, *15*, 162–182.
- [40] P. R. Taylor in *European Summerschool in Quantum Chemistry, Book III*, pp. 643–718, (Eds.: B. O. Ross, P.-O. Widmark), Lund University, **2000**.
- [41] W. Caminati, S. Melandri, P. Morechini, P. G. Favero, *Angew. Chem.* **1999**, *111*, 3105–3107; *Angew. Chem. Int. Ed.* **1999**, *38*, 2924–2925.
- [42] C. Tuma, A. D. Boese, N. C. Handy, *Phys. Chem. Chem. Phys.* **1999**, *1*, 3939–3947.
- [43] a) R. Hoffmann, *Tetrahedron Lett.* **1970**, 2907–2909; b) R. Hoffmann, W. D. Stohrer, *J. Am. Chem. Soc.* **1971**, *93*, 6941–6948;
- c) F. H. Allen, *Acta Crystallogr. Sect. B* **1980**, *36*, 81–96; d) F. H. Allen, *Acta Crystallogr. Sect. B* **1981**, *37*, 890–900; e) V. R. Pediredi, G. R. Desiraju, *Chem. Commun.* **1992**, 988–990; f) F. H. Allen, J. P. M. Lommerse, V. J. Hoy, J. A. K. Howard, D. R. Desiraju, *Acta Crystallogr. Sect. B* **1996**, *52*, 734–745.
- [44] S. Simon, M. Duran, J. J. Dannenberg, *J. Chem. Phys.* **1996**, *105*, 11024–11031.
- [45] a) B. Paizs, P. Salvador, A. G. Császár, M. Duran, S. Suhai, *J. Comput. Chem.* **2001**, *22*, 196–207; b) P. Salvador, B. Paizs, M. Duran, S. Suhai, *J. Comput. Chem.* **2001**, *22*, 765–786.

Received: September 29, 2003

Published online: May 11, 2004